RAPID COMMUNICATIONS

PHYSICAL REVIEW B VOLUME 44, NUMBER 8 15 AUGUST 1991-II

Scanning-tunneling-microscopy investigations of ternary graphite intercalation compounds

Stephen P. Kelty,* Zhong Lu, and Charles M. Lieber*
Departments of Chemistry and Electrical Engineering, Columbia University, New York, New York 10027
(Received 4 March 1991)

The surface structures of the stage-1 ternary graphite intercalation compounds KM_xC_4 (M_x=Hg, $H_{0.8}$) have been investigated using scanning tunneling microscopy. Constant-current and constant-height images of both materials exhibit superstructures in addition to the graphite atomic lattice. In the case of $KHgC_4$, a commensurate 2×2 and an incommensurate superstructure with a period of 8.9 ± 0.2 Å have been observed. Images of $KH_{0.8}C_4$ exhibit a one-dimensional superstructure with a 12.4 ± 0.2 Å period and a two-dimensional superlattice with a 14.5 ± 0.5 Å period. The 2×2 structure in $KHgC_4$ has been attributed to a modulation of the surface density of states by the periodic potential of the underlying intercalant. Possible explanations for these long-period superstructures observed in $KHgC_4$ and $KH_{0.8}C_4$ will be discussed.

The surface structure and electronic properties of graphite intercalation compounds (GICs) have been the focus of several recent scanning tunneling microscopy (STM) studies.[1-5] A goal of many of these studies has been to probe experimentally how the carbon-carbon interlayer interaction and the Fermi-surface size, which vary with intercalation, contribute to the carbon site asymmetry and the large vertical corrugations observed in STM images of graphite. It is also expected that STM may be an ideal technique to probe fundamental phenomena such as intercalant staging, order-disorder transitions, and Fermi-surface driven instabilities in these materials.

The majority of previous high-resolution STM studies have focused on the stage-1 alkali-metal GICs.[2-5] Images of LiC_6 were reported to exhibit commensurate 2×2 and $\sqrt{3}\times\sqrt{3}$ and incommensurate superlattices, however, the origin of these superstructures is uncertain.[2] Images of the stage-1 MC_8 (M=K, Rb, Cs) primarily show a commensurate 2×2 superlattice in addition to the hexagonal structure observed for graphite.[3] Since the 2×2 superlattice has the same structure as the intercalant layer it has been proposed that the STM images correspond to a modulation of the surface carbon layer density of states (DOS) due to the periodic potential of the underlying intercalant.[5] More recently, one-dimensional superlattices have also been observed in the stage-1 RbC_8 and CsC_8 materials.[4] It has been suggested that depletion of the intercalant from the surface region is required to observe the one-dimensional superlattice, however, it is not clear whether these superstructures have a structural (i.e., a different intercalant ordering) and/or electronic origin.

To understand the electronic and structural effects of intercalation and the physical properties of GICs better, we have been studying the ternary GICs ($M_xM'_yC_n$), and herein report the atomic resolution STM data on cleaved surfaces of stage-1 $KHgC_4$ and $KH_{0.8}C_4$. To date, high-resolution STM data has not been reported for the ternary GICs. These materials have, however, been intensely investigated and much is known about the structural and electronic properties of many of the ternary materials.[6] Structurally, the carbon/intercalant/carbon repeat structures of $KHgC_4$ and $KH_{0.8}C_4$ are similar: C/K-Hg_2-K/C and C/K-$H_{1.6}$-K/C, respectively [Fig. 1(a)].[6] Several different in-plane intercalant superlattices have, however, been reported for these materials. The major superlattice detected in diffraction studies of $KHgC_4$ is a 2×2 structure similar to that observed in KC_8 [Fig. 1(b)], although commensurate $2\times\sqrt{3}$ and $\sqrt{3}\times\sqrt{3}$ structures are also believed to exist as minority phases.[6,7] The in-plane intercalant structure of $KH_{0.8}C_4$ is not well established due to uncertainty in the H positions, however, both 2×2 and $2\times\sqrt{3}$ potassium superlattices have been reported.[8] Electronically, experimental[9-12] and theoretical[13,14] studies have addressed the fraction of charge transfer between the intercalant and graphite layers. These investigations suggest that the charge transfer per carbon atom is smaller in $KH_{0.8}C_4$ than $KHgC_4$, and, interestingly, that the Hg and H layers form metallic bands.[11,12]

The $KHgC_4$ and $KH_{0.8}C_4$ samples were prepared by heating highly oriented pyrolytic graphite (Union Carbide) and KHg or KH in evacuated pyrex tubes at 200–260 °C and 430 °C, respectively.[10,15] Stage-1 crystals were verified by x-ray diffraction measurements. The STM experiments were carried out in an inert atmosphere glove box ($[O_2],[H_2O]\leq1$ ppm) using a commercial STM.[16] Samples were cleaved in the glove box prior to

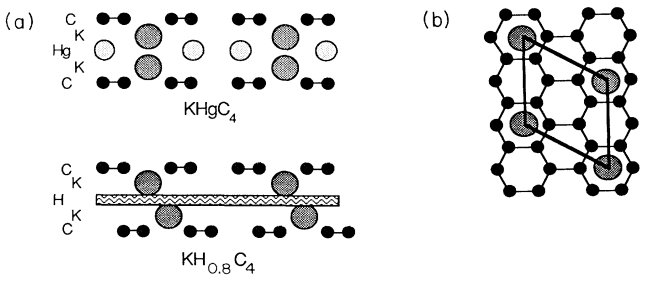

FIG. 1. (a) Cross-sectional view of $KHgC_4$ and $KH_{0.8}C_4$. The carbon layer stacking is *AA* in $KHgC_4$ and *AB* in $KH_{0.8}C_4$; the ordering of the hydrogen is not established. (b) Top-view illustrating the surface carbon layer and 2×2 superlattice of potassium in the second layer.

imaging and were stable for at least 8 h. Similar images were obtained with bias voltages between -750 and $+750$ mV, with tunneling currents between 0.5 and 5 nA, and in the constant height mode where the force between the sample and tip are approximately constant. Other experimental details have been described previously.[3,5]

A gray-scale image of $KHgC_4$ that is typical of those obtained over $\approx 90\%$ of the surface is shown in Fig. 2(a). Analysis of this real-space image shows that the characteristic feature is a $2\mathbf{a}\times 2\mathbf{a}$ superlattice ($\mathbf{a}=2.46$ Å) that is commensurate with the hexagonal graphite atomic structure. This commensurate 2×2 superlattice is also observed clearly in two-dimensional Fourier-transform (2DFT) power spectra of the images [Fig. 2(b)].[17] The amplitude of the 2×2 modulation, 0.4 ± 0.1 Å, is smaller than the 1-Å vertical corrugation observed for graphite with our experimental setup. In addition to the 2×2 superlattice, an incommensurate square superlattice with a period of 8.9 ± 0.2 Å has been observed over approximately 10% of the remaining surface [Fig. 3(a)]. The amplitude of the 8.9-Å period modulation 0.4 ± 0.1 Å is similar to that observed for the 2×2 superstructure. The square symmetry of this superlattice is not due to a nonlinearity in the piezo scanner or to thermal drift, since the graphite atomic lattice has an undistorted hexagonal symmetry. The superlattice in Fig. 3(a) exhibits a $4\pm 2°$ orientation relative to the atomic lattice. The orientation and symmetry of this incommensurate superlattice have also been verified by analysis of the 2DFT of the images [Fig. 3(b)]. Additionally, a second distinct orientation of this superlattice, $13\pm 2°$, has been detected in our images, although only one orientation (i.e., $4\pm 2°$ or $13\pm 2°$) is observed in any one image. Furthermore, the 8.9-Å period superlattice is observed immediately after cleaving samples and does not appear to evolve with time from the 2×2 superstructure, in contrast to recent results reported for RbC_8 and CsC_8.[4]

Images of $KH_{0.8}C_4$ show two long-period superlattices (Fig. 4). In approximately 70% of the images recorded to date we have observed a one-dimensional superstructure with a period of 12.4 ± 0.2 Å. The modulation direction of this superlattice is coincident with one of the graphite lattice vectors and has a period that corresponds within experimental error to a $5\mathbf{a}$ commensurate superstructure ($5\mathbf{a}=12.3$ Å). The remaining 30% of the images obtained on $KH_{0.8}C_4$ exhibit a near trigonal two-dimensional superlattice with a period of 14.5 ± 0.5 Å. Examination of the images and 2DFT of the real-space data demonstrated that this superlattice is rotated 30° relative to the graphite lattice [Fig. 4(c)]. We note that if the two-dimensional superstructure was resolved in only one direction, the resulting one-dimensional structure would have a

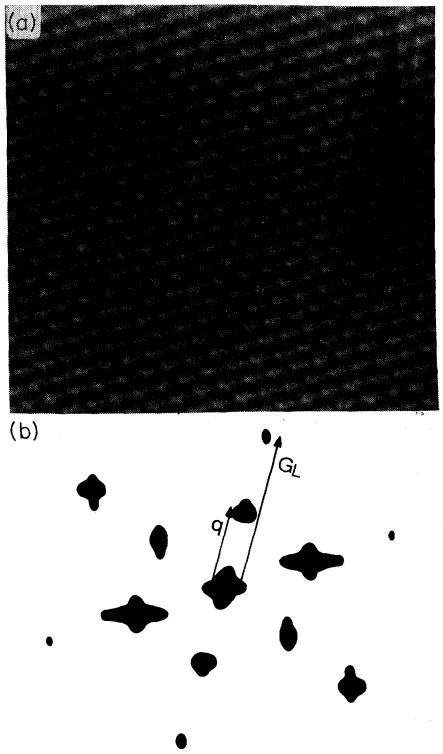

FIG. 2. (a) Unfiltered 100×100 Å^2 image of $KHgC_4$ that shows the 2×2 superstructure and graphite lattice. The image was recorded with a bias voltage of -15 mV and a tunneling current of 5 nA. (b) 2DFT power spectrum of (a) with one lattice vector (G_L) and superlattice vector (q) marked.

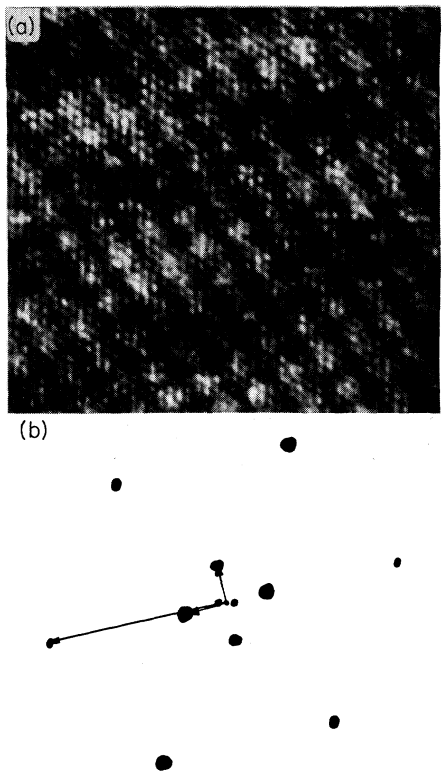

FIG. 3. (a) Unfiltered 100×100 Å^2 image of $KHgC_4$ that shows the 8.9 Å period square superlattice and the graphite lattice. The image was recorded with a bias voltage of 15 mV and a tunneling current of 4 nA. (b) 2DFT power spectrum which illustrates the square symmetry of the superlattice and its orientation ($\approx 4°$) relative to the graphite lattice.

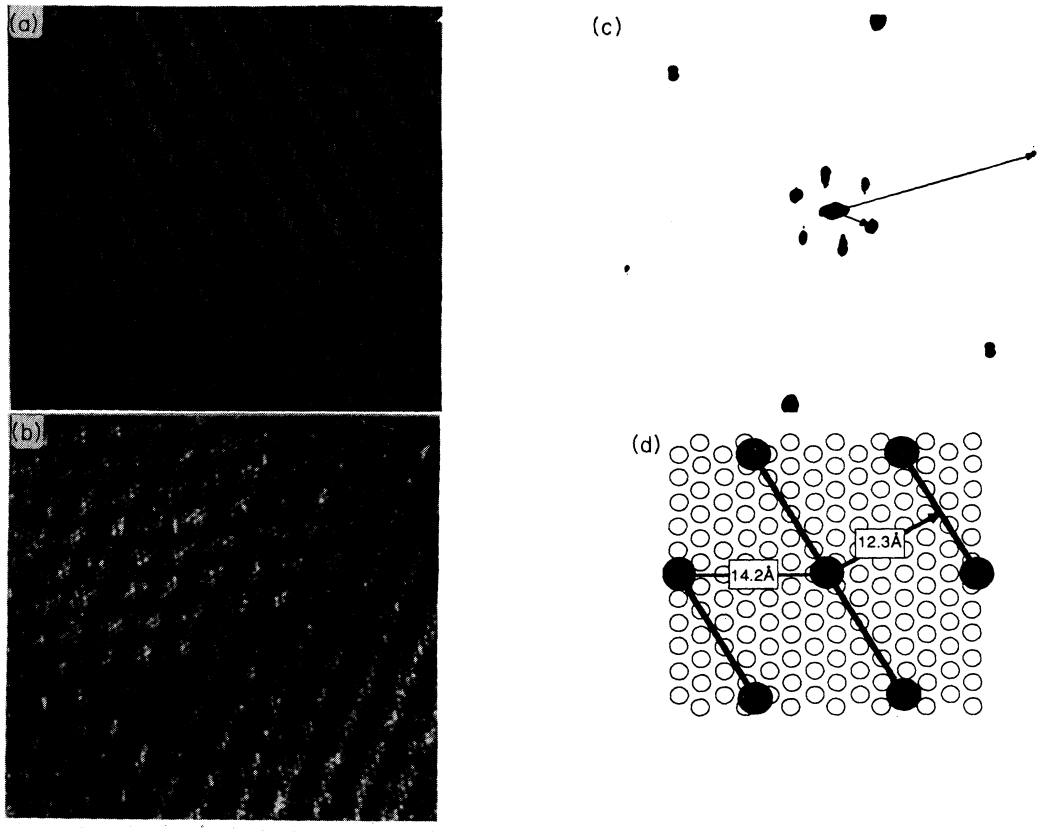

FIG. 4. Unfiltered 145×145 Å^2 images of $KH_{0.8}C_4$ illustrating (a) the 12.4 Å period one-dimensional superlattice and (b) the 14.5 Å period two-dimensional superlattice; the underlying graphite lattice is also visible in both images. The images were recorded with bias voltages (mV) or tunneling currents (nA) of $-\frac{50}{2}$ and $\frac{53}{2}$, respectively. (c) 2DFT power spectrum of (b) illustrating the hexagonal symmetry of the superlattice and its $\approx 30°$ orientation relative to the graphite lattice. (d) Schematic showing the relationship between the one-dimensional superstructure (heavy-black lines, 12.3 Å period), the two-dimensional superstructure (solid-black circles, 14.2 Å period), and the graphite lattice (open circles, 2.46 Å period).

modulation period of 12.3 Å along one of the graphite lattice vectors [Fig. 4(d)]. This is the same period and orientation found experimentally for the one-dimensional superlattice in Fig. 4(a). Hence, we suggest that both the one- and two-dimensional superstructures are the same, although the tip resolution is lower in the one-dimensional images.

There are several possible explanations to account for the superlattices observed in our images of $KHgC_4$ and $KH_{0.8}C_4$. We consider the 2×2 commensurate structure first. The 2×2 superlattice observed in images of $KHgC_4$ is virtually the same as that found in images of the MC_8 compounds. The degree of charge transfer to the carbon layers is lower in $KHgC_4$ vs KC_8 (0.063 vs 0.075),[8,18] and thus it is unlikely that the 2×2 superstructure is due to a Fermi-surface driven instability (e.g., a charge-density wave) since the periodicity should vary with the degree of charge transfer.[19] $KHgC_4$ and the MC_8 GICs do have the same 2×2 in-plane K (and Rb,Cs for MC_8) superstructure. Hence, a more likely explanation for the 2×2 superlattices observed in these different materials is that the periodic potential of the potassium ions directly beneath the surface carbon layer modulates the DOS of this surface layer to produce the observed 2×2 superstructure.[20] We favor this electronic explanation versus a structural one since the 2×2 modulation amplitude is similar in both compounds, although the compressibility of $KHgC_4$ is approximately two times greater than that of KC_8.[21] We have not observed this 2×2 modulation in images of $KH_{0.8}C_4$. Our x-ray photoelectron-spectroscopy (XPS) measurements demonstrate, however, that both $KHgC_4$ and $KH_{0.8}C_4$ have similar K concentrations at the surface. These XPS data thus indicate that the absence of 2×2 structure in the $KH_{0.8}C_4$ images is not simply due to a dilute intercalant layer.

Next we consider the long-period superstructures observed in $\approx 10\%$ of the $KHgC_4$ and 100% of the $KH_{0.8}C_4$ images. Anselmetti and co-workers have recently proposed a dilute intercalant layer to explain the one-dimensional superstructures they observed in images of RbC_8 and CsC_8.[4] Within the framework of their model we would expect the concentration of potassium to be lower in $KH_{0.8}C_4$ vs $KHgC_4$. However, our XPS measurements demonstrate that the surface potassium concentration is similar or even slightly higher in the $KH_{0.8}C_4$ materials. Although these XPS data cannot conclusively rule out the dilution model, they do suggest that the long-period superstructures that we observe have a different

origin.

An alternative explanation for the long-period modulations in $KH_{0.8}C_4$ and $KHgC_4$ is that they correspond to a charge density wave (CDW). Indeed, an inverse variation of wavelength with Fermi-surface size (i.e., the degree of charge transfer to the carbon layer) is one signature of a Fermi-surface driven CDW instability. For $KHgC_4$ and $KH_{0.8}C_4$, the fraction of charge transfer per carbon is -0.063 and -0.051, respectively,[18,22,23] consistent with the observed modulation periods. Since the detailed shape of the Fermi surfaces of these two compounds has not been determined, these data only indirectly support the existence of a CDW. We note, however, that a CDW in $KHgC_4$ has been suggested to suppress the superconducting transition in samples that do not contain pure α phase.[10,24] The α phase corresponds to the 2×2 intercalant layer structure, and thus we suggest that the minority phase proposed to support the CDW corresponds to the 8.9-Å period superlattice we observe over $\approx 10\%$ of the surface.[25] Furthermore, we note that superconductivity has not been detected in $KH_{0.8}C_4$ down to 70 mK despite favorable electron phonon coupling and density of states at the Fermi level.[8] If the 14.5 (12.4) Å superlattice corresponds to a CDW in $KH_{0.8}C_4$, then the absence of superconductivity is not unexpected since CDW formation will inhibit superconductivity.

In conclusion, we have used STM to characterize 2×2 and 8.9-Å period superlattices in $KHgC_4$ and 12.4 and 14.5 Å superlattices in $KH_{0.8}C_4$. The 2×2 superlattice has been consistently explained in terms of a modulation of the surface DOS by the periodic (2×2) potential of the underlying potassium ions. The long-period superstructures observed in images of $KHgC_4$ and $KH_{0.8}C_4$ have been tentatively attributed to a CDW with a wavelength dependent on the degree of charge transfer to the carbon layer. Further experiments designed to confirm or disprove the existence of a CDW, such as measurement of the CDW energy gap, are now essential to develop a better understanding of these fascinating materials.

C.M.L. acknowledges support of this work by the National Science, Packard, Sloan, and Dreyfus Foundations. The authors are grateful to A. W. Moore (Union Carbide) for the HoPG samples.

*Address correspondence to these authors at the Department of Chemistry and Division of Applied Sciences, Harvard University, Cambridge, MA 02138.

[1]S. Gauthier, S. Rousset, J. Klein, W. Sacks, and M. Belin, J. Vac. Sci. Technol. A **6**, 360 (1988).

[2]D. Anselmetti, R. Wiesendanger, and H. J. Guntherodt, Phys. Rev. B **39**, 11 135 (1989).

[3]Stephen P. Kelty and Charles M. Lieber, J. Phys. Chem. **93**, 5983 (1989); Phys. Rev. B **40**, 5856 (1989).

[4]D. Anselmetti, V. Geiser, G. Overney, R. Wiesendanger, and H. J. Guntherodt, Phys. Rev. B **42**, 1848 (1990).

[5]S. P. Kelty and C. M. Lieber, J. Vac. Sci. Technol. B **9**, 1068 (1991).

[6]S. A. Solin and H. Zabel, Adv. Phys. **37**, 87 (1988).

[7]G. Timp, B. S. Elman, R. Al-Jishi, and G. Dresselhaus, Solid State Commun. **44**, 987 (1982).

[8]T. Enoki, S. Miyajima, M. Sano, and H. Inokuchi, J. Mat. Res. **5**, 435 (1990).

[9]M. H. Yang, P. A. Charron, R. E. Heinz, and P. C. Eklund, Phys. Rev. B **37**, 1711 (1988).

[10]A. Chaiken, M. S. Dresselhaus, T. P. Orlando, G. Dresselhaus, P. M. Tedrow, D. A. Neumann, and W. A. Kamitakahara, Phys. Rev. B **41**, 71 (1990).

[11]Seiichi Miyajima, Masashi Kabasawa, Takehiko Chiba, Toshiaki Enoki, Y. Maruyama, and H. Inokuchi, Phys. Rev. Lett. **64**, 319 (1990).

[12]S. B. DiCenzo, P. A. Rosenthal, H. J. Kim, and J. E. Fischer, Phys. Rev. B **34**, 3620 (1986).

[13]N. A. W. Holzwarth, Q. Wang, and S. D. Had, Phys. Rev. B **38**, 3722 (1988).

[14]Seiji Mizuno and Kenji Nakao, Phys. Rev. B **41**, 4938 (1990); **40**, 5771 (1989).

[15]D. Guerard, C. Takoudjou, and F. Rousseaux, Synth. Met. **7**, 43 (1983).

[16]Nanoscope, Digital Instruments, Inc., Santa Barbara, CA.

[17]The 2DFT power spectra of one image that did not show the 2×2 superlattice did exhibit a $(\sqrt{3}\times\sqrt{3})R30$ superlattice. This latter structure has been observed infrequently by electron diffraction (Ref. 7), and is consistent with a high-local intercalant concentration.

[18]G. Timp, T. C. Chieu, P. D. Dresselhaus, and G. Dresselhaus, Phys. Rev. B **29**, 6940 (1984).

[19]J. A. Wilson, F. J. DiSalvo, and S. Mahajan, Adv. Phys. **24**, 117 (1975).

[20]XPS data show that composition of the surface region of $KHgC_4$ is close to stoichiometric and does not correspond to KC_8.

[21]H. J. Kim, H. Mertwoy, T. Koch, J. E. Fischer, D. B. McWhan, and J. D. Axe, Phys. Rev. B **29**, 5947 (1984).

[22]T. Enoki, N. C. Yeh, S. T. Chen, and M. S. Dresselhaus, Phys. Rev. B **33**, 1292 (1986).

[23]Preliminary studies of stage-2 $KH_{0.8}C_8$, which has a charge transfer per carbon of -0.03, show a superlattice with a period of ≈ 19 Å. The additional increase in modulation period relative to the stage-1 compounds is consistent with the CDW explanation.

[24]L. E. DeLong and P. C. Eklund, Synth. Met. **5**, 291 (1983).

[25]Samples that are prepared under conditions that yield nearly pure α phase rarely exhibit the 8.9-Å period superlattice.

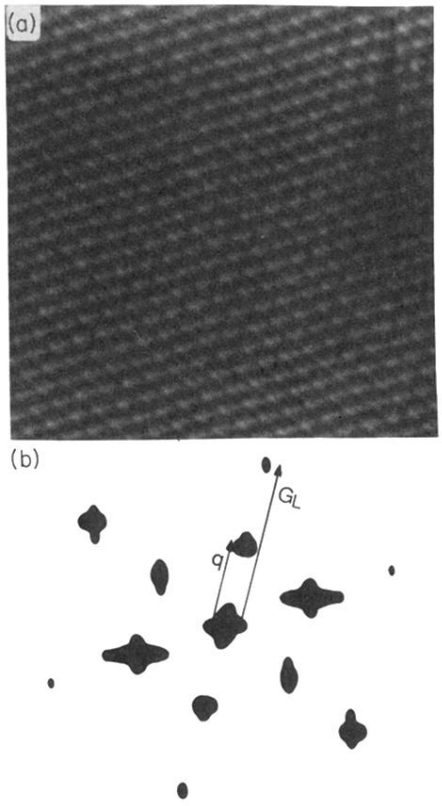

FIG. 2. (a) Unfiltered 100×100 Å^2 image of $KHgC_4$ that shows the 2×2 superstructure and graphite lattice. The image was recorded with a bias voltage of -15 mV and a tunneling current of 5 nA. (b) 2DFT power spectrum of (a) with one lattice vector (G_L) and superlattice vector (q) marked.

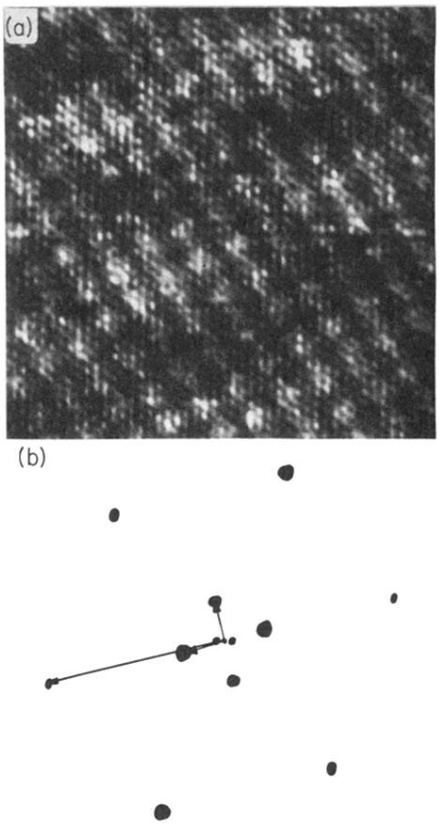

FIG. 3. (a) Unfiltered 100×100 Å^2 image of $KHgC_4$ that shows the 8.9 Å period square superlattice and the graphite lattice. The image was recorded with a bias voltage of 15 mV and a tunneling current of 4 nA. (b) 2DFT power spectrum which illustrates the square symmetry of the superlattice and its orientation ($\approx 4°$) relative to the graphite lattice.

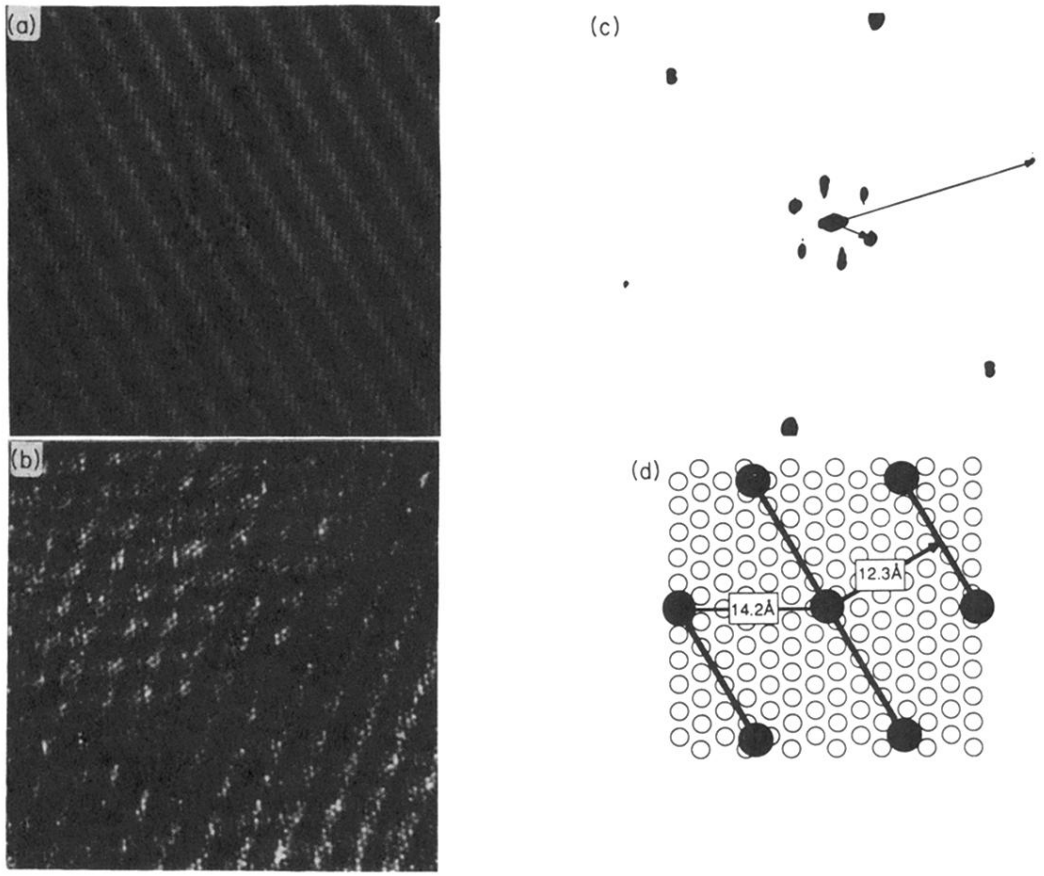

FIG. 4. Unfiltered 145×145 Å^2 images of $KH_{0.8}C_4$ illustrating (a) the 12.4 Å period one-dimensional superlattice and (b) the 14.5 Å period two-dimensional superlattice; the underlying graphite lattice is also visible in both images. The images were recorded with bias voltages (mV) or tunneling currents (nA) of $-\frac{50}{2}$ and $\frac{53}{2}$, respectively. (c) 2DFT power spectrum of (b) illustrating the hexagonal symmetry of the superlattice and its $\approx 30°$ orientation relative to the graphite lattice. (d) Schematic showing the relationship between the one-dimensional superstructure (heavy-black lines, 12.3 Å period), the two-dimensional superstructure (solid-black circles, 14.2 Å period), and the graphite lattice (open circles, 2.46 Å period).